Equilibrium of an elastically confined liquid drop

Hyuk-Min Kwon,[1] Ho-Young Kim,[1,a)] Jérôme Puëll,[2] and L. Mahadevan[2,b)]
[1]*School of Mechanical and Aerospace Engineering, Seoul National University, Seoul 151-744, Republic of Korea*
[2]*School of Engineering and Applied Sciences, Harvard University, Cambridge, Massachusetts 02138, USA*

(Received 11 November 2007; accepted 2 March 2008; published online 7 May 2008)

When a liquid drop is confined between an elastic plate and a rigid substrate, it spreads spontaneously due to the effects of interfacial forces, eventually reaching an equilibrium shape determined by the balance between elastic and capillary effects. We provide an analytical theory for the static shape of the sheet and the extent of liquid spreading and show that our experiments are quantitatively consistent with the theory. The theory is relevant for the first step of painting when a brush is brought down on to canvas. More mundanely, it allows us to understand the stiction of microcantilevers to wafer substrates occurring in microelectromechanical fabrication processes. © *2008 American Institute of Physics*. [DOI: 10.1063/1.2913512]

I. INTRODUCTION

The first and often crucial step in Chinese calligraphy and certain forms of painting such as pointillism is the bringing of a wet brush or other soft paint-bearing element to the canvas. This leads to a spontaneous spreading of a drop of paint due to the effects of interfacial forces. Here we analyze this simple process to determine the shape of the brush and the drop as a function of the various parameters that characterize the problem. This study complements our previous work on the capillary rise of a liquid between two elastic plates, a problem motivated by the uptake of paint by a soft elastic brush.[1,2] However, there is a qualitative difference between the elastocapillary rise problem treated in Ref. 2 and that considered here since volume conservation rather than gravity determines the final equilibrium shape of the drop and plate. This type of problem also arises in some technological situations associated with microelectromechanical systems where a common process involves thin microstructures such as cantilever beams or bridges that can be fabricated by a surface micromachining process called wet release etch. In this process, a sacrificial layer deposited on a substrate, over which a structural material is deposited and patterned, is removed by wet etching to leave an overhanging structure. Upon post-etch rinsing, surface tension pulls in the compliant beams as the rinsing solution dries. If the bending stiffness of the beam is small (in a way that we shall quantify), it is brought into contact with the substrate and they may adhere firmly together, a phenomenon generally called stiction.[3] Indeed, this process is a simple instance that shows how the combination of interfacial forces and nonequilibrium kinetics such as that induced by drying can lead to the self-assembly of soft simple elements into complex structures.

Here we focus on a minimal system consisting of a drop that lies between two plates of length, L, and width, w, separated by a distance, H, which is much smaller than L and w. If the drop volume $\tilde{\Omega} \gg H^3$, then volume conservation implies that it spreads into an elliptical drop having the length of approximately $\tilde{\Omega}/Hw$ with deviations from the shape arising due to the capillary effects along the edge of the drop. If one or both plates are flexible and hydrophilic, capillary forces associated with the meniscus curvature lead to a negative pressure in the liquid causing the gap between the sheets to be modulated. For a relatively short and stiff sheet, the liquid spreads slightly more due to this effect and is accompanied by a slight decrease in the gap between the sheets. However, when the sheets are long and flexible, they can deform substantially and even stick to each other leading to a qualitatively different behavior. To understand these at a simple level, we start with the relatively stiff regime. When a sheet of length, L, thickness, t, density, ρ_s, and bending stiffness, B, is deflected through a distance, δ, due to surface tension, σ, balancing the torque exerted on the sheet, $B\delta/L^2$, with the capillary torque, $\sigma\Omega L/(H-\delta)^2$, yields $\delta \sim \sigma\Omega L^3/BH^2$, where the two-dimensional volume, $\Omega=\tilde{\Omega}/w$. Denoting the extent of spreading by l_m, volume conservation gives $\Omega \sim (H-\delta)l_m$ so that l_m is modified to $l_m=l_r(1-k/\eta)^{-1}$, where $l_r=\Omega/H$. Here $\eta=(l_a/L)^2(H/L)^2(HL/\Omega)$ is a parameter that characterizes the ratio of elastic and capillary forces up to geometric factors, and $l_a=(B/\sigma)^{1/2}$ is the adhesion or bending length.[4] The constant k is of order unity, showing how the effects of plate stiffness appear perturbatively to modify the extent of drop spreading. We note that as $\eta \to \infty$, we recover $l \sim l_r$. As η decreases, on the other hand, the effects of capillary adhesion become important so that the sheet deforms more, leading to a higher degree of spreading. When $\eta \ll 1$, the sheet eventually sticks to the rigid plate starting from its free end, so that the quantity of interest is the dry length l_d. Minimizing the sum of the elastic energy of the deformed sheet BH^2/l_d^3 and the interfacial energy $\sigma(L-l_d)$ yields $l_d \sim (B/\sigma)^{1/4}H^{1/2} \sim (l_aH)^{1/2}$. In the following, we formulate and solve a free boundary problem to understand the quantitative dependence of liquid spreading and sheet shape on the various problem parameters to complement these simple scaling estimates.

a)Electronic mail: hyk@snu.ac.kr.
b)Electronic mail: lm@seas.harvard.edu.

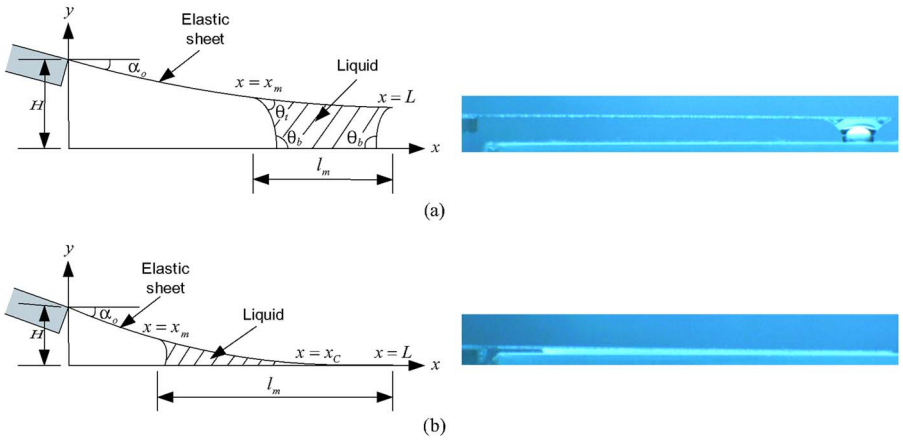

FIG. 1. (Color online) Schematics and experimental images of the sheet and liquid drop. (a) The glass sheet, 36.2 mm long and 1.85 mm apart from the substrate at the clamped end, is relatively stiff so that the free end is separated. (b) The same glass sheet 0.28 mm apart from the substrate at the clamped end, is relatively soft so that the end is in contact with the substrate. In both the experimental images, the same volume of the ethylene glycol drop is used and the substrate is parafilm.

II. THE FREE BOUNDARY PROBLEM: FORMULATION, SOLUTION, AND EXPERIMENTAL CORROBORATION

We consider a liquid drop in equilibrium between a rigid horizontal flat plate and a flexible sheet clamped at an angle α_0, as shown in Fig. 1. When the clamping distance $H \ll L$, we may use linear plate theory to describe its deformation $h(x)$ (Ref. 5)

$$Bh''''(x) = q(x), \tag{1}$$

where B is the bending stiffness per unit width of the sheet, $h' \equiv dh/dx$, and $q(x)$ is the force per unit area on the sheet.

A. Spreading under a stiff plate with a separated end

For $\eta \geq O(1)$, i.e., in the relatively stiff regime, the sheet is in contact with liquid over an unknown length, $l_m = L - x_m$, while its free end is still some distance from the bottom plate as shown in Fig. 1(a). We neglect the effect of gravity on both the drop and the elastic plate. The conditions for this are (i) the Bond number of the drop $\mathrm{Bo} = \rho g H^2/\sigma \ll 1$ and (ii) the torque due to weight $M_g \sim \rho_s g t L^2$ is small compared with the torque due to surface tension $M_s \sim \sigma \Omega L/H^2$, i.e., $L \ll \sigma\Omega/\rho_s g t H^2$. When a water drop and the glass sheets used for the computation in Fig. 2 are considered, Bo is below 0.09 and the ratio M_g/M_s is of the order of 10^{-2}. In micromachining processes to fabricate 1 μm-thick silicon nitride beams overhanging 100 μm from the substrate, the numbers are even smaller, Bo and M_g/M_s being of the order of 10^{-3} and 10^{-5}, respectively.

Then the relative pressure in the liquid is $-\sigma/R_0$, where R_0 is the radius of curvature of the menisci. Then the pressure distribution over the entire range of x can be simply written as $q = -(\sigma/R_0)\mathcal{H}(x - x_m)$, where $\mathcal{H}(.)$ is the Heaviside function. Substituting into Eq. (1) yields

$$Bh'''' = -\frac{\sigma}{R_0}\mathcal{H}(x - x_m), \tag{2}$$

To complete the formulation of the problem, we need some boundary conditions. As the plate is clamped at $x=0$, it follows that $h(0)=H$ and $h'(0)=\tan\alpha_0$. At the other end, the sheet is free of torques but is subject to a transverse shear force due to surface tension so that $h''(L)=0$ and $Bh'''(L) = \sigma \sin\theta_L$, where θ_L is the contact angle of the liquid with the end of the sheet. These four boundary conditions must be supplemented by matching conditions at the meniscus, $x = x_m$, given by the continuity of the deflection, the slope, and the curvature of the sheet, i.e., $[h]=[h']=[h'']=0$, where $[A] = \lim_{\epsilon\to 0}\{A(x_m+\epsilon) - A(x_m-\epsilon)\}$. However, there is a jump in the transverse shear force across $x=x_m$ due to surface ten-

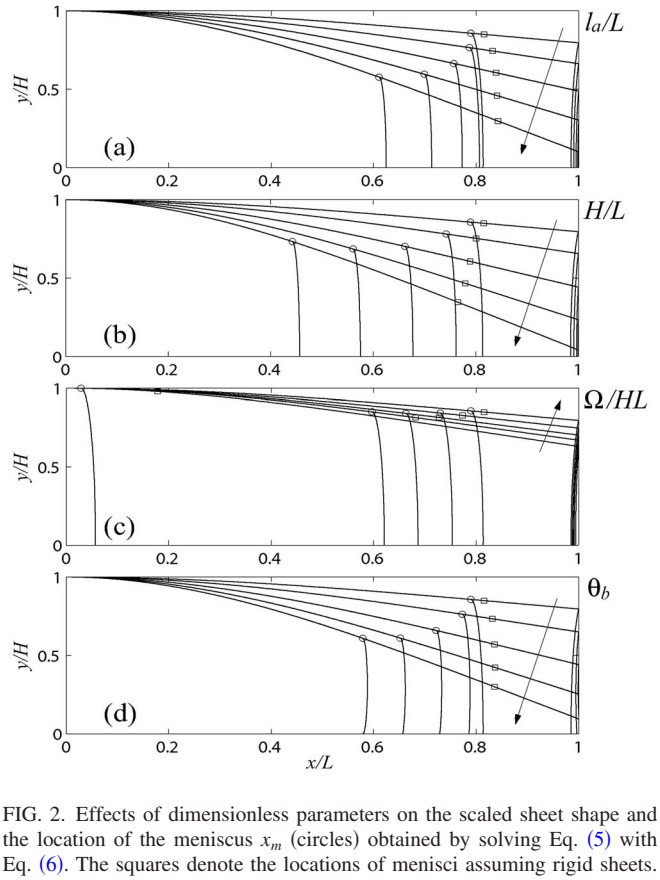

FIG. 2. Effects of dimensionless parameters on the scaled sheet shape and the location of the meniscus x_m (circles) obtained by solving Eq. (5) with Eq. (6). The squares denote the locations of menisci assuming rigid sheets. For purposes of comparison, the uppermost curve in each case corresponds to the following parameter values: $l_a/L=19.3$, $H/L=0.0293$, $\Omega/HL=0.141$, and $\theta_b=87°$. The contact angle $\theta_t=0°$ for all the cases. These are consistent with the parameter values for water spreading under the thin hydrophilic sheet of length $L=27.3$ mm and $B=0.022$ Nm separated by a height $H=0.8$ mm from a rigid substrate having the contact angle $\theta_b=87°$ with water. (a) l_a/L decreases in the direction of the arrow taking the values 19.3, 17.6, 16.9, 16.7, and 16.5. (b) H/L decreases in the direction of the arrow taking the values 0.0293, 0.0256, 0.0234, 0.0220, and 0.0201. (c) Ω/HL decreases in the direction of the arrow taking the values 0.778, 0.275, 0.229, 0.183, and 0.141. (d) θ_b decreases in the direction of the arrow taking the values 87°, 60°, 40°, 30°, and 0°.

sion so that $[Bh''']=\sigma \sin \theta_t$, where θ_t is the contact angle of the meniscus with the sheet. To determine the unknown meniscus location, x_m, and the radius of curvature, R_0, as well as the eight constants of integration resulting from Eq. (2), we need two more conditions in addition to the earlier eight boundary and matching conditions. One is provided by the conservation of the liquid volume, Ω, which for the two-dimensional geometry considered here reads

$$\int_V dxdy = \Omega. \tag{3}$$

The last condition comes from the description of the left-hand meniscus whose top and bottom contact angles are prescribed. Since gravitational effects are neglected, the left-hand meniscus is a part of circle with the radius R_0. Then $h_m=h(x_m)$ can be related to R_0 by simple geometrical consideration as

$$h_m = R_0(\cos \theta_b + \cos \varphi), \tag{4}$$

where θ_b is the contact angle of the liquid with the substrate and φ is the angle between the horizontal and the tangent to the top of the left-hand meniscus thus given by $\varphi=\theta_t-\alpha_m$. Here α_m is the slope of the sheet at $x=x_m$, thus $\tan \alpha_m = h'(x_m)$. The right-hand meniscus is directly deduced from the shape of the left-hand one as the pressure in the drop is a constant when gravitational effects are neglected. The contact angle of the right-hand meniscus with the sheet is free as the drop is assumed to be pinned to the edge of the sheet.

To make the equations and boundary conditions dimensionless, we use the scaled variables $x=L\hat{x}$, $y=H\hat{y}$, and $h=H\hat{h}$, so that the complete boundary value problem reads, upon dropping the hats, as

$$h'''' = \frac{L^4}{l_a^2 H R_0}\mathcal{H}(x-x_m) \tag{5}$$

subject to the conditions

$$\begin{aligned}
&h(0)=1,\\
&h'(0)=L\tan\alpha_0/H,\\
&h''(1)=0,\\
&h'''(1)=L^3\sin\theta_L/Hl_a^2,\\
&[h]=0,\\
&[h']=0,\\
&[h'']=0,\\
&[h''']=L^3\sin\theta_t/Hl_a^2,\\
&\Omega/HL=\int dxdy,\\
&Hy_m/R_0=\cos\theta_b+\cos(\theta_t-\alpha_m).
\end{aligned} \tag{6}$$

We see that the shapes of the sheet and menisci depend on three dimensionless parameters, namely l_a/L, H/L, and Ω/HL in addition to the contact angles θ_t and θ_b. Here we note that x_m and R_0 are not parameters but unknown quantities to be obtained by the boundary value problem. Integrating Eq. (5) yields a polynomial shape of the sheet with eight integration constants. These constants, the unknown meniscus location x_m and its shape R_0, are obtained by using ten conditions (6) to yield closed-form expressions for $h(x)$, using MATLAB.

In Fig. 2 we show the dimensionless shape of the sheet $y(x)$ as a function of the dimensionless parameters: l_a/L, H/L, Ω/HL, and θ_b. On comparing the location of the left meniscus with that for a rigid plate, we see that a higher degree of spreading occurs when the liquid has a large interfacial tension and the sheet is soft and long (low l_a/L), while the separation at the clamped end is small (low H/L). Not surprisingly, a large amount of liquid (high Ω/HL) with small contact angles spreads more. Lowering l_a/L and H/L and increasing Ω/HL correspond to decreasing the dimensionless stiffness η. As η decreases further, the sheet becomes relatively more flexible leading to contact with the bottom plate. This changes the problem qualitatively due to a change in the boundary conditions, a case treated in next section.

To compare these results with experiments, we start with a glass cover slip cleaned with piranha solution to make them almost perfectly wettable by water and ethylene glycol (EG). The sheet width $w=4$ mm and the thickness $t=150$ μm, respectively, and its length $L\in[19.1\ 38.7]$ mm. The drop volume $\Omega\in[0.858\ 13.74]$ mm^3. For the bottom plates, we used Parafilm M laboratory sealing film (PF: American National Can, Chicago, IL) having an equilibrium contact angle $\theta_b=89°$ with EG and polycarbonate having the contact angle $\theta_b=87°$ with water. Figure 3(a) shows that the scaled spreading length, l_m/L, increases as the scaled height, H/L, decreases, revealing good agreement between the theory and the experiments. For small gaps, i.e., low values of H/L, liquid spreading is greatly enhanced for soft elastic plates, i.e., small η, as compared with that under rigid plates. In Fig. 3(b), we compare the experimental measurements with the scaling introduced earlier, $l_m \sim l_r(1-k/\eta)^{-1}$, which is also reasonably good for small values of $1/\eta$.

B. Spreading under a soft sheet with a contacting end

If we increase the sheet length, or decrease its flexural rigidity or gap height to make $\eta \ll 1$, surface tension causes the sheet to touch the bottom plate at the free end. Figure 4 shows the change of sheet shapes on increasing the sheet length L while maintaining the gap height H and the liquid volume Ω. When the sheet length increases to, say, L_1, the sheet touches the bottom, and the formulation of the resulting free boundary problem changes slightly since the boundary condition corresponding to the force due to surface tension on the right side of the sheet $h'''(1)=L^3 \sin \theta_L/Hl_a^2$ is replaced by the kinematic condition $h(1)=0$. As η becomes

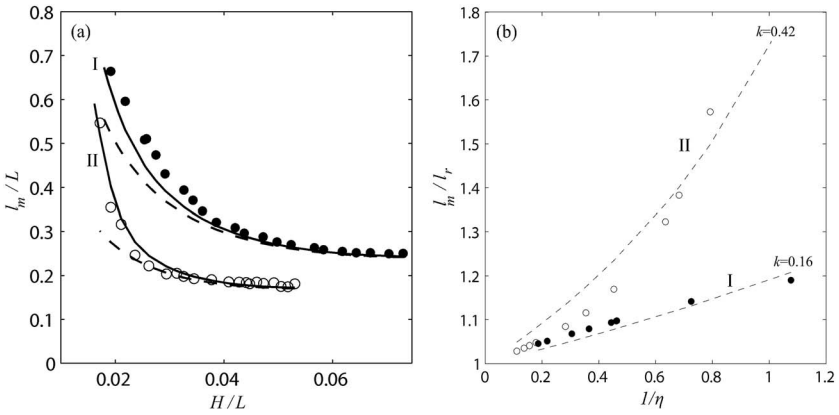

FIG. 3. (a) Comparison of experimental results and theoretically predicted spreading length l_m obtained by solving Eqs. (5) and (6). The broken lines are the spreading length under rigid plates. (b) Replotting the experimental results and the scaling law $l_m/l_r \sim 1/(1-k/\eta)$ with an adjustable parameter k also shows reasonable agreement. Line I and filled circles are for $l_a/L=27.6$ and $\theta_b=89°$, and the rightmost filled circle in (a) corresponds to $\Omega/HL=0.129$. Line II and open circles are for $l_a/L=20.8$ and $\theta_b=89°$, and the rightmost open circle in (a) corresponds to $\Omega/HL=0.066$.

even smaller, the angle between the plates at their contacting ends, still at $x=L$, decreases until eventually it vanishes when the sheet length is, say, $L=L_2$, leading to smooth tangential contact between the plates along a line (line III in Fig. 4). Still further increase in the sheet length, with $L>L_2$, then causes the contact line between the sheets to move to an unknown location $x=x_c$. In this new regime, there are two unknown locations: the wet-dry meniscus x_m and the location of the contact line x_c beyond which the sheet and the bottom plate are effectively in contact [see Fig. 1(b)]. When $L>L_2$, the quantity of interest is the size of the dry and wet regions, and the sheet shape for $0<x<x_c$ is independent of the length of the entire sheet. The governing Eq. (5) still holds for $0<x<x_c$ and the boundary conditions at $x=0$ and the matching conditions at $x=x_m$ are identical to the foregoing formulations. At $x=x_c$, $h(x_c)=h'(x_c)=0$ consistent with tangentially smooth contact. Furthermore, assuming a thin intercalating layer of liquid even in the region $x_c<x<L$, where the solid sheets are in nominal contact, yields $h''(x_c)=0$.[2] Solving the differential Eq. (5) with the additional conditions earlier gives the sheet shape and the two unknown locations x_m and x_c.

Figure 5(a) shows the experimental and theoretical results for the transition between the separated-end regime and the contacting-end regime. As the sheet height decreases, the separated-end solution ceases to be valid when the sheet contacts the substrate, entering the contacting-end regime (path A in the figure). On the other hand, when raising the sheet from the end-contact configuration, we experimentally find that the sheet does not detach from the substrate following the path A. Instead the end-contacting regime persists until the path B. This is because the shear force acting at the free end of the sheet continues to be upward (negative y''') until the sheet is separated from the substrate. If we consider the additional contribution of surface tension acting along the width of the drop, this accounts for the persistence of the end-contacting configuration between paths A and B. Indeed such a mechanism has been proposed qualitatively to explain the release etch processing for microfabrication that is responsible for the stiction behavior of a microcantilever under which a drying liquid drop exerts a surface tension force toward the substrate.[6] Adding the surface tension force acting at both sides of the sheet (-2σ) divided by its width to $q(x)$ in Eq. (1), the right-hand side of Eq. (2) becomes $-\sigma(1/R_0+2/w)\mathcal{H}(x-x_m)$. Here we have approximated the surface tension at the sides as acting vertically. This yields the wetted length as a function of H/L as shown by the dotted line in Fig. 5(a). The shear force acting at the free end of the sheet calculated using this modified model vanishes at the point denoted as a cross. This agrees well with the experimentally found transition point indicated by the path B. For other ranges, including the surface tension acting at the sides of the sheet changed values of l_m/L little (less than 5%). We note that the spreading length l_m increases with the height decrease much more sensitively in the contacting-end regime than in the separated-end regime.

Figure 5(b) shows reasonable agreement between experiment and theory for the transition between the end-contact regime and tangentially smooth-contact regime. The figure also shows the aforementioned scaling law $l_m/L=1-l_d/L=1-k(l_aH)^{1/2}/L$, with the adjustable constant $k=1.7$, which agrees well with the experiments.

III. DISCUSSION

Our quantitative theory and experiments for the spreading of an elastically confined drop has probed the simplest elements of the configuration of the sheet and drop as a function of the fluid volume, the length of the sheet, and its distance from the substrate as well as the stiffness of the sheet and surface tension of the liquid. We have shown that there are three distinct configurations of the sheet depending on the value of the scaled stiffness of the sheet which combines geometric and physical parameters. Our focus has been

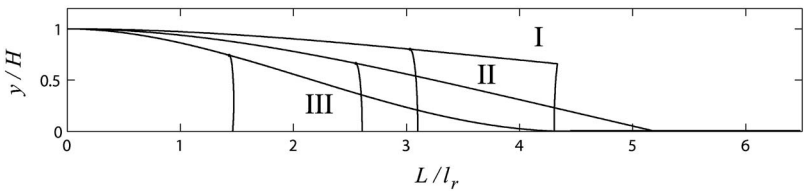

FIG. 4. Theoretically predicted beam shapes and meniscus locations when $L<L_1$ (line I), $L_1<L<L_2$ (line II), and $L>L_2$ (line III).

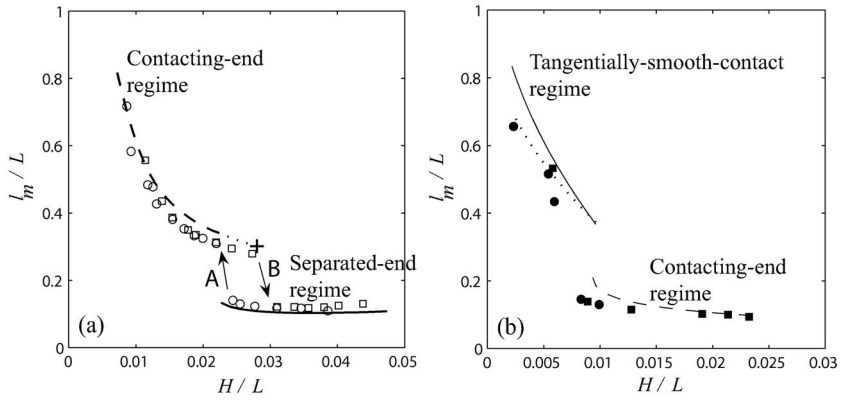

FIG. 5. Theoretical and experimental results for three regimes. (a) Transition between the separated-end regime and the contacting-end regime. The solid and broken lines are theoretical solutions of the separated and contacting end regimes, respectively, obtained by varying H while l_a/L is maintained at 14.1. The dotted line is from the modified model that considers the surface tension acting at the sides of the sheet. Open circles and squares are the experimental results measured while decreasing and increasing H, respectively. The parameter $\Omega/HL=0.044$ for the rightmost symbol, which changes as H varies although Ω and L are constants. (b) Transition between the contacting-end regime and the tangentially smooth-contact regime. The broken and solid lines are theoretical solutions of the contacting-end and tangentially smooth-contact regimes, respectively, obtained by varying H while l_a/L is maintained at 14.1. Filled circles and squares are the experimental results measured while decreasing and increasing H, respectively. The parameter $\Omega/HL=0.028$ for the rightmost symbol, which changes as H varies although Ω and L are constants. The dotted line is from the scaling law. In all the cases of (a) and (b), $\theta_b=89°$.

on two-dimensional configurations; much remains to be done for more complex geometries associated with, say, the multiple hairs of a paint brush. This problem may serve as a precursor toward a qualitative theory of how more complex structures might arise from these simple interactions when modified by kinetic processes such as drying.

We now conclude by adding some discussions on how this problem can be extended to more complex but relevant situations. When the drop does not touch the free end initially but rather located between the clamped and the free ends, the drop will eventually move to the free end to reach the equilibrium. This is because the pressure in the liquid around the meniscus near the clamped end (having a smaller interface curvature) is higher than the pressure near the free end (having a larger interface curvature) thus propels the drop toward the free end. Hence, the current formulation can still be used for the situation considered. When the sheet width is reduced to a comparable size to the gap height ($w - R_0$), the three-dimensional effect comes into play. A mere inclusion of the surface tension force acting at both sides of the sheet as discussed earlier to explain the dotted line in Fig. 5(a) can result in good estimates for the shapes of the sheet and the drop provided that the interface curvature along the side is neglected. Since the contact angle at the side is not simply defined due to the fact that the angle is now formed at the solid edge, considering the interface profile along the side involves a much more complex study. In general, for narrow sheets, additional effects of the surface tension forces that pull the sheet downward tend to enhance both the sheet deformation and the drop spreading. Similar three-dimensional effects are to be considered for circular filaments, a geometry of most real brushes, for which our present study can provide qualitative estimates for the two-dimensional filament deformation and the degree of liquid spreading.

ACKNOWLEDGMENTS

J.P. was supported by a grant from Ecole Polytechnique, Paris that allowed him to complete a stage at Harvard University in 2004, which marked the beginning of the project. H.Y.K. gratefully acknowledges support from Korea Science and Engineering Foundation (Grant No. R01-2006-000-10444-0) administered via SNU-IAMD.

[1] J. Bico, B. Roman, L. Moulin, and A. Boudaoud, Nature (London) **432**, 690 (2004).
[2] H.-Y. Kim and L. Mahadevan, J. Fluid Mech. **548**, 141 (2006).
[3] S. D. Senturia, *Microsystem Design* (Kluwer, Boston, MA, 2001).
[4] A. E. Cohen and L. Mahadevan, Proc. Natl. Acad. Sci. U.S.A. **100**, 12141 (2003).
[5] L. D. Landau and E. M. Lifshitz, *Theory of Elasticity*, 3rd ed. (Butterworth-Heinemann, Oxford, 1986).
[6] T. Abe, W. C. Messner, and M. L. Reed, J. Microelectromech. Syst. **4**, 66 (1995).